Journal of Applied Mechanics Vol.8, pp.225-231 (August 2005) JSCE

Numerical solution of the Navier-Stokes equations for incompressible flow in porous media with free surface boundary

Nenad JACIMOVIC*, Takashi HOSODA**, Kiyoshi KISHIDA*** and Marko IVETIC****

*PhD Student, Department of Urban Management, Kyoto University (606-8501, Kyoto)
**Professor, Department of Urban Management, Kyoto University (606-8501, Kyoto)
*** Associate Professor, Department of Urban Management, Kyoto University (606-8501, Kyoto)
****Professor, Faculty of Civil Engineering, Belgrade University (Serbia & Montenegro)

The paper presents numerical solution of the three dimensional Navier-Stokes equations for complex flow domains consisting of fluid and porous regions with free surface boundary. Flow in both regions is described by single set of conservation equations, extending the momentum equation for porous regions by additional viscous drag term according Darcy law. Free surface kinematics is "tracked" by Volume of Fluid method. Firstly the model is verified by comparision with numerical solution of Laplace equation for simple free surface flow through vertical dam. Good result agreements are observed. Application on realistic problems is presented on two cases. First case considers problem of pressure redistribution process around a deep tunnel excavation in low-conductivity porous media and second considers flow under and through porous, partially submerged bridge.

Key Words: Navier- Stokes equations, porous media, numerical solution

1. Introduction

Many practical problems involve simultaneous bulk fluid flow and flow through the porous media. Applications include ground water / surface water pollution and flow problems, geophysical systems, oil production, etc. Penetration of fluid from reservoir into some kind of porous media is also significant phenomena in various fields of industry (e.g. ink jet technologies), where the accompanying process of heat transfer can also be of interest.

In practice, problem involves coupling of equations describing fluid region flow (Navier-Stokes equations) and flow through porous media, usually described by some form of Darcy-law equation. Due to different structure of these equations, some empirical conditions on the interface between regions are required. Beavers and Joseph[1], amongst the first, proposed a "slip-flow" condition at the interface. Based on experimental results they concluded that slip velocity is proportional to the shear rate on the interface.

After Wooding[2], who introduced convective inertia term in the Darcy law equation, resembling in that way Navier-Stokes equations, Beckermann et al.[3] solved coupled equations (for fluid and porous region) numerically in two dimensions. Their set of governing equations under steady state condition introduces binary parameter, through which transition from porous to fluid region is achieved. On the other hand, inertia effects in the porous region were introduced using Brinkman and Forchheimer extensions of Darcy law equation.

At the same time, major efforts have been made on the development of numerical methods to obtain accurate solution of Navier-Stokes equations for flows with the free surface boundary. Standard advection techniques for convection problems can be applied for free surface "capturing", but inevitably lead to diffusion or oscillations. Although powerful techniques were proposed to limit diffusion or unstable behavior (e.g. see Reference [4]), they can not guarantee the sharp, non oscillatory interface.

The first method, capable for free surface "tracking", was the well-known Marker and Cell (MAC) method, proposed by Welch et al.[5]. In this method massless Lagrangian markers are advected by the local velocity field, where distribution of markers determines position of free surface.

Later, several volume tracking techniques were proposed[6], where the volume fraction of fluid is tracked in the computational cells which contain free surface. Among others is the Volume of Fluid (VOF) method[7], which is utilized in this paper, and will be briefly described in the following section.

The purpose of this paper is to present numerical model for incompressible, laminar flows in porous, as well as in fluid region, with free surface boundary. Continuity of velocities and stresses across the interface of two regions is assumed. The presented model can be applied to wide variety of flow problems with porous media as a part or as the whole flow domain. Two such applications are herein presented .

The reminder of paper is organized as follows. In the next section, an overview of computational method is given. In the third section, the model is verified by comparison with numerical solution of Laplace equation for a simple flow problem in porous media. Model application on realistic flow problems is presented in the following two sections: In Section 4, the case of pressure redistribution over deep tunnel excavation is analyzed, where analytical solution is derived, and in Section 5 model's application is demonstrated on flow under permeable, partially submerged bridge. The paper is concluded in Section 6.

2. Outline of numerical model

Governing equations for laminar flow of incompressible fluid in the fluid region, as well as in the rigid, homogeneous porous media region can be formulated as:

$$\frac{\partial}{\partial x_i}\left[(1-c)U_i\right]=0\,, \tag{1}$$

$$\rho(1-c)\frac{\partial U_i}{\partial t}+\rho(1-c)U_j\frac{\partial U_i}{\partial x_j}=\rho(1-c)g_i$$

$$-(1-c)\frac{\partial p}{\partial x_i}+\frac{\partial}{\partial x_j}\left[\rho(1-c)\nu\left(\frac{\partial U_i}{\partial x_j}+\frac{\partial U_j}{\partial x_i}\right)\right]-\rho g\frac{(1-c)^2}{K}U_i \tag{2}$$

where x_i is the spatial co-ordinate, t time, ρ the fluid density, c the volumetric concentration of particles, p pressure, K the hydraulic conductivity, ν the fluid viscosity and U_i pore velocity.

Flow resistance of porous media in equation (2) is introduced by Darcy-law term, and can be extended to non-Darcy fluid flows by introduction of nonlinear terms. Considering continuity of flow, pore fluid velocity and Darcy (or seepage) velocity are related as:

$$(1-c)U_i=V_i \tag{3}$$

where V_i is Darcy velocity.

Equations (1) and (2) are discretized by the finite volume (FV) method on the full-staggered computational grid, where velocity components are defined on the cell faces and scalar variables are defined at the cell centers.

Pressure and velocity field at new time steps are calculated by iterative procedure using the Highly Simplified Marker and Cell (HSMAC) method[8]. Iterative procedure consists of two steps. Firstly the predicted value of velocity is calculated using second-order Adams-Bashforth scheme:

$$\left(U_i^{n+1}\right)^{r+1}=U_i^n+\frac{\delta t}{\rho(1-c)}\left(1.5F^n-0.5F^{n-1}\right)-\frac{\delta t}{\rho}\left(\frac{\partial p}{\partial x_i}\right)^r \tag{4}$$

where $\left(U_i^{n+1}\right)^{r+1}$ is the velocity at current time step (n+1), at (r+1)-th iteration and δt is time step. F^n in equation (4) is expressed as follows:

$$F^n=-\rho(1-c)U_j^n\frac{\partial U_i^n}{\partial x_j}+\rho(1-c)g_i$$

$$+\frac{\partial}{\partial x_j}\left(\rho(1-c)\nu\frac{\partial U_i^n}{\partial x_j}\right)-\rho g\frac{(1-c)^2}{K}U_i^n\,, \tag{5}$$

and accordingly, F^{n-1} denotes the same expression for time step (n-1).

After obtaining predicted velocity field, the divergence for each cell is computed. Then, using (6) and (7) the pressure field is corrected in order to satisfy equation (1):

$$\left(p^{n+1}\right)^{r+1}=\left(p^{n+1}\right)^r-\frac{\omega D^{r+1}}{2\delta t\left(\frac{1}{\delta x_1^2}+\frac{1}{\delta x_2^2}+\frac{1}{\delta x_3^2}\right)}\,, \tag{6}$$

$$D^{r+1}=\frac{\partial}{\partial x_i}\left[(1-c)(U_i)^{r+1}\right] \tag{7}$$

where ω is relaxation coefficient, δx_i is size of computational cell in the 'i' direction. As the values at the first iteration, pressures and velocities from the previous time step are used. Iterations are repeated until value |D| satisfy the given criteria at every computational cell.

The convective inertia term in equation (4) is described using the QUICK scheme [9].

Free surface kinematics (in a case of unconfined flow) is simulated by extension of Volume of Fluid (VOF) method, here adapted for flow in porous media as follows.

After obtaining the divergence-free velocity field at the new time step, convective equation

$$\frac{\partial(1-c)F}{\partial t}+\frac{\partial}{\partial x_i}\left[(1-c)FU_i\right]=0\,, \tag{8}$$

is solved, where $(1-c)F$ represents portion of cell occupied by the fluid (cell saturation). Donor-acceptor technique is used to advect "fluid volume" as combination of first order upwind and downwind fluxes[7].

At the interfaces of fluid and porous region, fluxes are calculated using the lower value (1-c) of the donor and acceptor cell, meaning that no more fluid can cross the interface than donor can physically provide, or acceptor to receive. The same is applied in cases of inhomogeneous porous media, with interfaces of different types of material.

In the original paper[7], equation (8) is solved in two-dimensional space. However, there was no mention whether it is solved simultaneously in both directions, or by direction split method. In this sudy, the direction split method is applied with alternate change of direction order at each time step.

3. Model verification

In order to verify the presented (FV) model with (VOF) method for free surface tracking, results of numerical solution based on equations (1) and (2) are compared with results of finite element (FEM) numerical solution of governing equation for 2D Darcy flow (Laplace equation) for homogeneous, isotropic porous media in vertical plane.

The models are applied on the problem of seepage through vertical dam, after sudden decrease of downstream water level as shown in Figure 1.

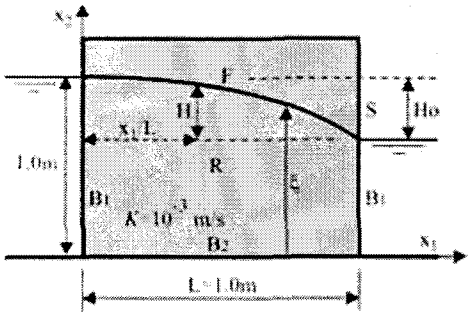

Fig. 1: Seepage through vertical dam, boundary conditions

Outline of the finite element model

This initial boundary value problem, for the rigid porous media considered here, can be described by the following set of equations[10]:

$$\frac{\partial}{\partial x_i}\left(K\frac{\partial h}{\partial x_i}\right)=0\,, \qquad \text{on R} \tag{9}$$

$$h(x_i,0) = h_o(x_i) \quad (10)$$

$$\xi(x_i,0) = \xi_o(x_i) \quad (11)$$

$$h(x_i,t) = H_1(x_i,t) \quad \text{on } B_1 \quad (12)$$

$$h(x_i,\xi,t) = \xi(x_i) \quad \text{on F} \quad (13)$$

$$K(\frac{\partial h}{\partial x_i})n_i = -(1-c)\frac{\partial \xi}{\partial t}n_2 \quad \text{on F} \quad (14)$$

$$K(\frac{\partial h}{\partial x_i})n_i = 0 \quad \text{on } B_2 \quad (15)$$

$$h = x_2 \quad \text{on S} \quad (16)$$

Here, h is total head, ξ elevation of the free surface from the bottom boundary, H_1 prescribed head, R the flow domain, B_1 prescribed head boundary, B_2 prescribed flux boundary (zero flux is used), F the free surface boundary and S the seepage face.

Position of the free surface at new time step is calculated by iteration. Each iteration consists of two steps[10]. At the first step equation (9) is solved for prescribed head conditions at the free surface and seepage face from the previous iteration. At the end of this step, nodal fluxes on the seepage face are calculated and used at the second step together with fluxes on the free surface boundary from (14). In second step (9) is solved again, but now with prescribed fluxes on the free surface and seepage face. At the end of second step, the mesh is deformed in order to satisfy condition (13).

Iterations are repeated until difference between calculated pressure head on the free surface and position of free surface satisfy the given criteria.

Flow domain is discretized by linear quadrilateral elements. Figure 2 shows converged finite element mesh for one denivelation case. Finer mesh discretization resulted to change of computed free surface levels by less than 1%.

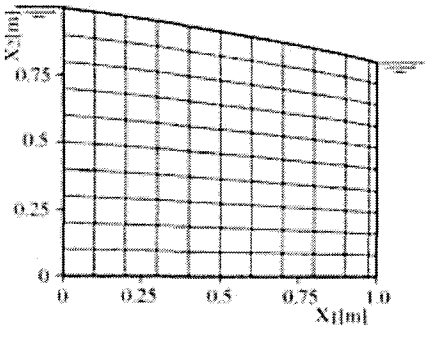

Fig. 2: Seepage through vertical dam, finite element mesh (Ho = 0.2m)

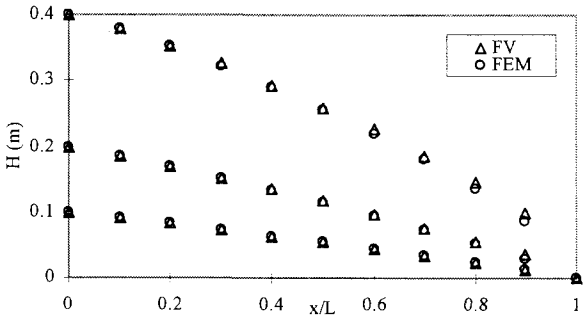

Fig. 3: Calculated free surface levels for three different denivelation cases: Ho=0.1, 0.2 and 0.4m (FV-finite volume model, FEM-finite element model)

Results and discussion

After obtaining steady conditions, results for three denivelation cases are compared on Figure 3.

Good agreement between the results suggests that (VOF) method can adequately track free surface movement in porous media. Convective inertia term, in case of flow with small gradients is negligible, but as gradient increase this term becomes more significant and the calculated surface levels slightly differ from (FEM) solution. In such cases, this gives better reconstruction of free surface boundary.

As it was described above, finite element approach requires special treatment of the seepage face. Here, particular problem represents intersection point of free surface and seepage face boundary, because calculation of nodal flux at this point includes both boundaries and error has effect on the whole domain. Several approximations are suggested to treat this problem. One of them is to place this point in the line with the two nearest nodes on F[10], which is used here.

In finite volume model, the seepage face boundary is naturally included by imposing zero pressure at the cells on this boundary. Considering other boundaries in (FV) model, constant pressure is imposed on B_1, and no flow condition on B_2.

4. Study case: flow towards tunnel excavation in low conductivity porous media

The presented finite volume model is applied on the problem of pressure redistribution process over deep tunnel excavation in low-conductivity porous media. Intention was to test the performance of the model in highly unsteady conditions.

Figure 4 schematically shows the flow domain. Boundary conditions are constant piezometric heads on the vertical domain boundaries, and zero pressure on the walls of excavation. Initially, hydrostatic pressure distribution is assumed everywhere.

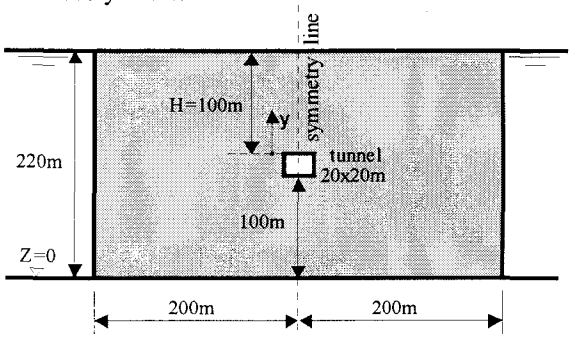

Fig. 4: Study case of tunnel excavation in porous media (K=1.0e-8 m/s, (1-c)=0.5)

Results of simulation are compared with analytical solution of pressure distribution along symmetry line above the excavation (described below) and finite element solution of Darcy-law equation in vertical plane. Here, the same finite element model is used as described in previous section.

Analytical solution of pressure redistribution

The analytical solution is based on the assumption that vertical velocity distribution above tunnel excavation is linear:

$$v = v_o(t)\left(-\frac{y}{H}+1\right) \tag{17}$$

Here v is vertical velocity, v_o is vertical velocity at the tunnel boundary (y=0), y is vertical coordinate (positive upward), H is water height above tunnel excavation and t is time.

Neglecting the third term on the right side of equation (2), and assuming homogeneous, rigid porous media, momentum equation in the y direction can be written as:

$$\frac{\partial v}{\partial t}+v\frac{\partial v}{\partial y}=-g-\frac{1}{\rho}\frac{\partial p}{\partial y}-C_y v \tag{18}$$

with $C_y=\frac{g(1-c)}{K}$.

Substituting (17) into (18) yields:

$$\left(\frac{dv_o}{dt}-\frac{v_o^2}{H}+C_y v_o\right)\left(1-\frac{y}{H}\right)=-g-\frac{1}{\rho}\frac{\partial p}{\partial y} \tag{19}$$

which can be integrated from y=0 (p=0) to y=H (p=0) to obtain:

$$H\frac{dv_o}{dt}=v_o^2-HC_y v_o-2gH \tag{20}$$

This can be written as:

$$\frac{dv_o}{(v_o-\alpha)(v_o-\beta)}=\frac{dt}{H} \tag{21}$$

where:

$$\alpha=\frac{HC_y}{2}-\sqrt{\left(\frac{HC_y}{2}\right)^2+2gH} \tag{22}$$

and

$$\beta=\frac{HC_y}{2}+\sqrt{\left(\frac{HC_y}{2}\right)^2+2gH} \tag{23}$$

Now, solution of (20) can be easily derived as:

$$v_o(t)=\frac{\alpha-\beta e^{-\frac{t}{bH}}}{1-e^{-\frac{t}{bH}}} \tag{24}$$

in which:

$$b=\left(2\sqrt{\left(\frac{HC_y}{2}\right)^2+2gH}\right)^{-1} \tag{25}$$

It should be noted that from (24) $v_o \to \alpha$ when $t \to \infty$.

Substitution of (24) into (19) and after integration, one obtains expression for the pressure distribution as:

$$-g\varphi(y,t)=\left\{\frac{e^{\left(\frac{-t}{bH}\right)}}{bH\left(1-e^{\left(\frac{-t}{bH}\right)}\right)}\left[\beta-\frac{\alpha-\beta e^{\left(\frac{-t}{bH}\right)}}{1-e^{\left(\frac{-t}{bH}\right)}}\right]-\frac{1}{H}\left[\frac{\alpha-\beta e^{\left(\frac{-t}{bH}\right)}}{1-e^{\left(\frac{-t}{bH}\right)}}\right]^2+C_y\left[\frac{\alpha-\beta e^{\left(\frac{-t}{bH}\right)}}{1-e^{\left(\frac{-t}{bH}\right)}}\right]\right\}\left(y-\frac{y^2}{2H}\right) \tag{26}$$

Regarding the numerical model, due to existence of symmetry line, one can model only half of flow domain showed in Figure 4. Along this line no flow boundary condition should be imposed.

Discretized flow domain for finite volume model with boundary conditions is showed in Figure 5.

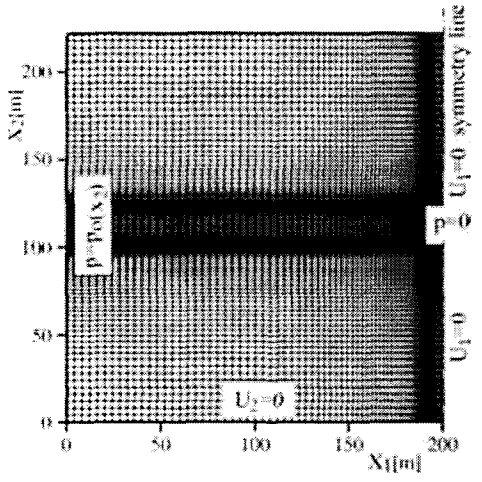

Fig. 5: Flow around tunnel excavation: discretization with boundary conditions

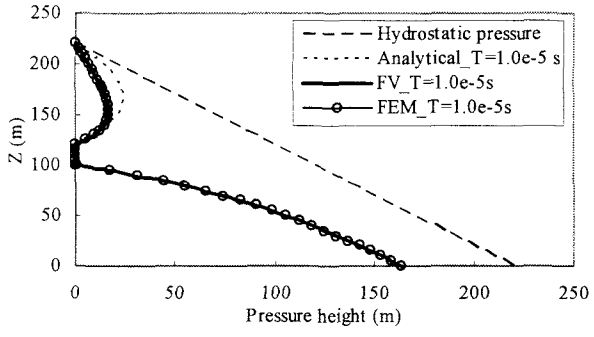

Fig. 6: Results of pressure distribution along the symmetry line: FV -finite volume model, FEM-finite element model

Figure 6 shows several results of calculation. In cases of low conductivity porous media, steady state flow is achieved in a very long time, but quasi-steady conditions, where pressure distribution does not change significantly, occur rapidly. This rapid pressure redistribution is observed from FV model results. Analytical solution confirm the results of FV model. Nevertheless, the assumption of linear vertical velocity distribution (analytical solution) is not adequate, except near the excavation, which explains the difference between numerical and analytical solution.

Finite element solution of Laplace equation (9) with the same boundary conditions as showed in Figure 5, produced identically pressure distribution curve as quasi-steady solution of FV model (Figure 6).

It can be concluded that, in obtaining quasi-steady pressure distribution, inertia term is negligible.

Case of tunnel with less permeable lining

Similar analysis is conducted for the case of tunnel excavation lined by less permeable material (Figure 7).

Since the width of lining is small comparing to tunnel depth (H), velocity through lining can be assumed equal as velocity v_o.

Hence, velocity distribution can be expressed as:

$$v = v_o(t), \quad 0 \le y \le H_1 \tag{27a}$$

$$v = v_o(t)\frac{H}{H-H_1}\left(1-\frac{y}{H}\right), \quad H_1 \le y \le H \tag{27b}$$

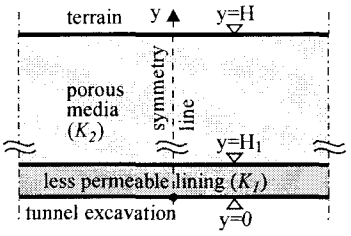

Fig. 7: Schematic cross-section of tunnel excavation lined by less permeable material

Substituting (27) into (18) gives:

$$\frac{dv_o}{dt} + C_{y1}v_o = -g - \frac{1}{\rho}\frac{\partial p}{\partial y}, \quad 0 \le y \le H_1 \tag{28a}$$

$$\left(\frac{dv_o}{dt} - \frac{v_o^2}{(H-H_1)} + C_{y2}v_o\right)\frac{H}{H-H_1}\left(1-\frac{y}{H}\right) = -g - \frac{1}{\rho}\frac{\partial p}{\partial y},$$

$$H_1 \le y \le H \tag{28b}$$

Integrating along the symmetry line, one obtains:

$$(H+H_1)\frac{dv_o}{dt} = v_o^2 - v_o\left[2C_{y1}H_1 + C_{y2}(H-H_1)\right] - 2gH \tag{29}$$

which gives solution as:

$$v_o(t) = \frac{\alpha - \beta e^{-\frac{t}{b(H+H_1)}}}{1-e^{-\frac{t}{b(H+H_1)}}} \tag{30}$$

where

$$\alpha = \frac{\left[2C_{y1}H_1 + C_{y2}(H-H_1)\right]}{2} - \left[\left\{\frac{\left[2C_{y1}H_1 + C_{y2}(H-H_1)\right]}{2}\right\}^2 + 2gH\right]^{-2}, \tag{31}$$

$$\beta = \frac{\left[2C_{y1}H_1 + C_{y2}(H-H_1)\right]}{2} + \left[\left\{\frac{\left[2C_{y1}H_1 + C_{y2}(H-H_1)\right]}{2}\right\}^2 + 2gH\right]^{-2}, \tag{32}$$

$$b = \frac{1}{(\beta-\alpha)}. \tag{33}$$

Substitution of (30) into (28) and after integration gives pressure distribution along symmetry line above tunnel excavation as:

$$-g\varphi(y,t) = \left\{\frac{w}{b(H+H_1)(1-w)}\left[\beta - \frac{(\alpha-\beta w)}{(1-w)}\right] + C_{y1}\left(\frac{\alpha-\beta w}{1-w}\right)\right\}y, \quad 0 \le y \le H_1 \tag{34a}$$

$$-g\varphi(y,t) = \left\{\frac{w}{b(H+H_1)(1-w)}\left[\beta - \frac{(\alpha-\beta w)}{(1-w)}\right] - \frac{1}{(H-H_1)}\left[\frac{(\alpha-\beta w)}{(1-w)}\right]^2 + \frac{(\alpha-\beta w)}{(1-w)}C_{y2}\right\}\frac{H}{H-H1}\left[(y-H_1) - \frac{\left(y^2-H_1^2\right)}{2H}\right] + \left\{\frac{w}{b(H+H_1)(1-w)}\left[\beta - \frac{(\alpha-\beta w)}{(1-w)}\right] + C_{y1}\left(\frac{\alpha-\beta w}{1-w}\right)\right\}H_1, \quad H_1 \le y \le H \tag{34b}$$

in which

$$w = e^{\left(-\frac{t}{b(H+H_1)}\right)}, \quad C_{y1} = \frac{g(1-c)}{K_1}, \quad C_{y2} = \frac{g(1-c)}{K_2}.$$

Figure 8 shows results of computation. For numerical solution, the same discretization and boundary conditions are used as shown on Figure 5.

As expected, quasi steady pressure distribution is obtained rapidly. Analytical solution slightly differs from numerical, due to linear velocity assumption. However, as from diagram it can be seen, it can give a solid approximation for practical purposes.

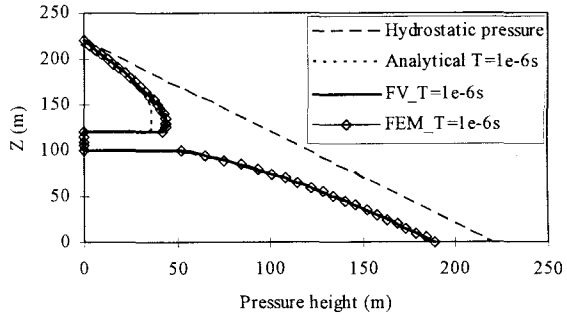

Fig. 8: Results of pressure distribution along the symmetry line for the case of tunnel with less conductivity lining (K_1=10^{-10}m/s, K_2=10^{-8}m/s, H_1=0.3m) FV-finite volume model, FEM-finite element model

It is interesting to note that pressure distribution above tunnel excavation in this case is almost the same as long as the ratio of conductivities of porous media and lining material is constant. Particularly, if one neglects inertia terms from equations (28), with the procedure shown above, one can derive expression for piezometric head at the interface of the lining (y=H_1) as:

$$\varphi_1 = \frac{H}{1 + \frac{H+H_1}{2H_1}\frac{C_{y2}}{C_{y1}}} \tag{35}$$

which means that it depends only of ratio of hydraulic conductivities, not on their absolute value.

5. Study Case 2: Flow through and under partially submerged porous bridge

Model application will be demonstrated on the case of flow under/through partially submerged porous bridge. Schematic diagram of flow domain with boundary conditions is shown in Figure 9.

At the upstream boundary, constant discharge is prescribed. On the downstream boundary, specified free surface level is applied with vanishing velocity gradient. Initially uniform water level is imposed. Of interest is discharge distribution under and through the bridge.

In all calculations, hydraulic conductivity of bridge material is considered as high (clean, coarse pebble, or a truss bar structure). It is observed that in cases of hydraulic conductivity of order 10^{-2} m/s or less, for given boundary conditions, almost all of the discharge flows under the bridge.

Figure 10 shows characteristic dependence of discharge under the bridge for steady conditions as function of opening height and conductivity of porous material.

Flow distribution is highly dependent on porous conductivity for small openings, while influence decreases with increment of the opening height. For openings higher than 50% of downstream water depth, flow under the bridge is over 95% in all cases.

The calculated temporal velocity fields with free surface elevations, for one case of boundary conditions, are shown in Figure 11.

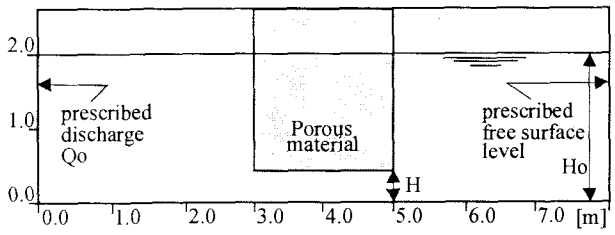

Fig. 9: Flow under/through porous bridge, initial and boundary conditions

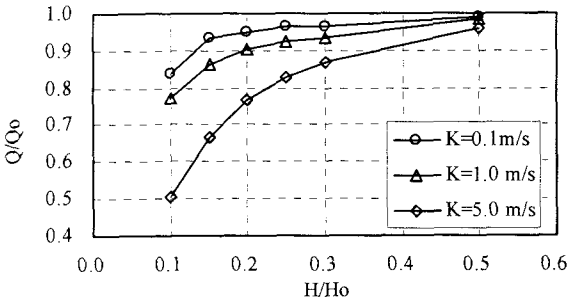

Fig. 10: Calculated nondimensional discharge under the bridge (Qo=40L/s/m, Ho=2m, (1-c)=0.5)

It is evident that velocity field through the bridge is dependent on process of vortex development at the downstream side.

However, further experimental research is required to explain this phenomenon in more detail.

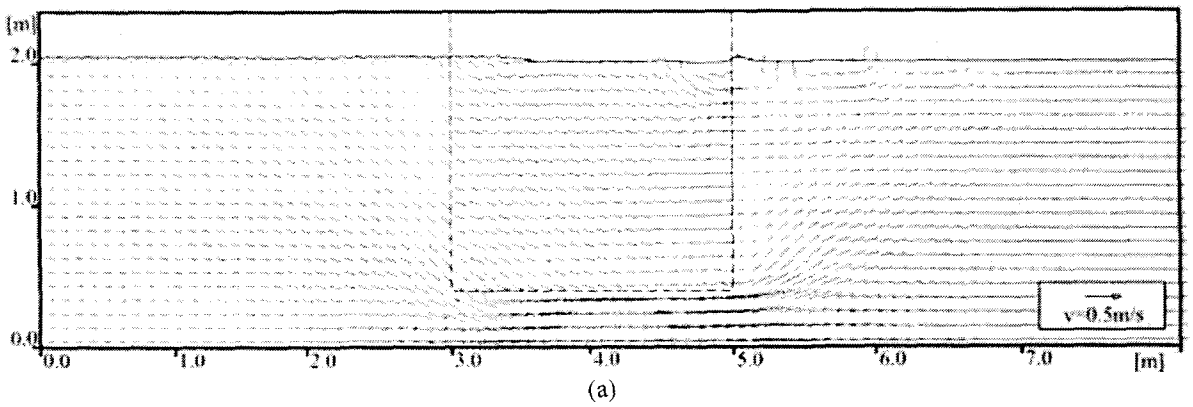

(a)

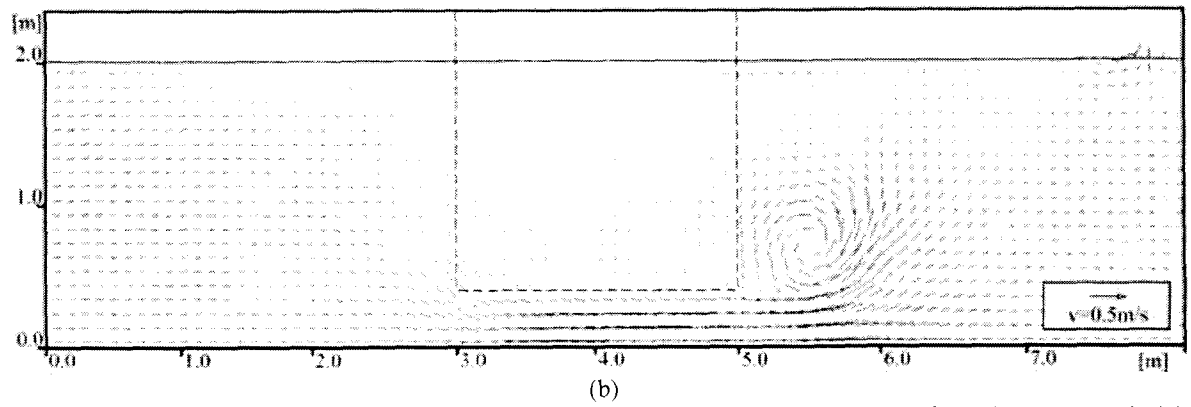

(b)

Fig. 11: Simulation of flow under porous, submerged bridge: (a) 4.0s and (b) 7.0 s after start of simulation Qo=200L/s/m, Ho=2.0m, H=0.4m, K=1.0m/s, (1-c)=0.5)

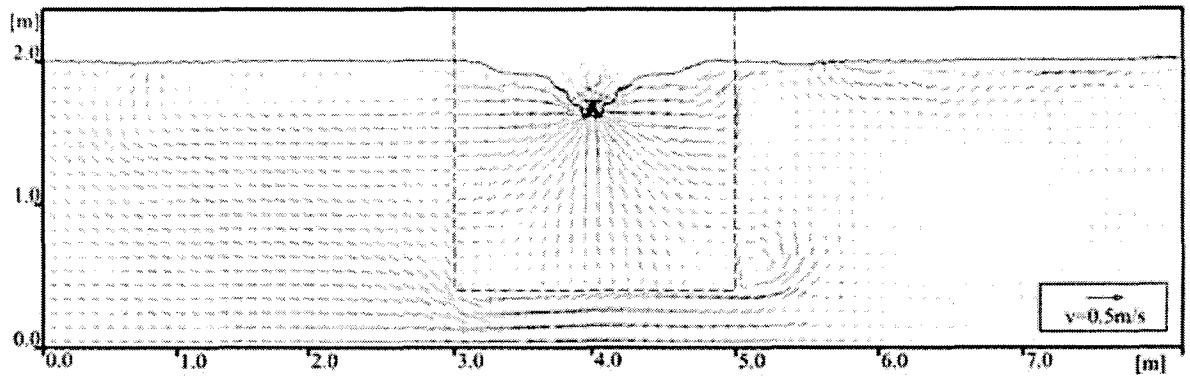

Fig. 12: Simulation of flow under porous submerged bridge with drain, 5s after start of simulation (Qo=200L/s/m, Ho=2.0m, H=0.4m, K=1.0m/s, (1-c)=0.5)

Velocity field, in the case of existence of drainage in the bridge, is showed in Figure 12. In this case flow through the bridge is dominantly oriented to the drain.

Figure 13 shows temporal change of water level along the channel for the drainage case, with sudden decrease of downstream water level from 2.2 m to 1.8 m. It can be seen that sudden changes in water levels produced no problems in the treatment of boundaries between fluid and porous regions.

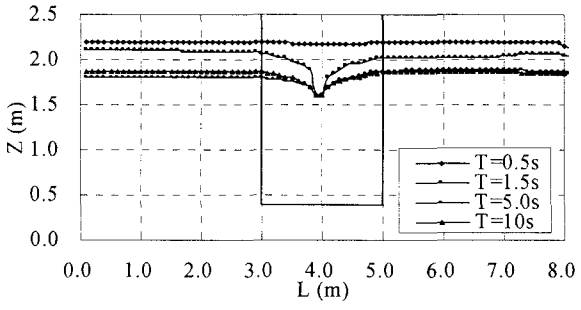

Fig. 13: Calculated temporal free surface elevations (Qo=200L/s/m, Ho=1.8m, H=0.4m, H_{init}=2.2m, K=1.0m/s,. Drain bottom level = 1.6m)

6. Conclusions

A numerical model has been developed for simulation of flows in complex domains which include fluid and porous regions with free surface boundaries. Assuming continuity of velocities and stresses at interfaces of different regions, single set of governing equations is used. To include viscous drag in the porous region, momentum equation has been extended by Darcy term. Although the model is fully 3D functional, in present study is applied only on 2D flow problems.

Model is successfully validated for flow in porous media by comparison with numerical solution of Laplace equation for the problem of seepage through vertical dam. Small effect of convective term in momentum equation is observed.

Application is also demonstrated on the problem of pressure redistribution process over deep tunnel excavation in a low conductivity porous media. Analytical solution of unsteady pressure distribution along symmetry line above the tunnel is derived under assumption of linear vertical velocity distribution. Analytical solution confirmed temporal behavior of this process. However, some disagreement in pressure heights values is observed, which can be explained by poor assumption of velocity distribution. Comparison with finite element model results showed excellent agreement.

Model is also applied on the flow problem in complex flow domain consisting of fluid and porous regions. It was observed that for small openings, flow is highly dependent on porous conductivity, while for openings of 50% of downstream boundary water level, under flow exceeds 95%. To verify the presented simulation results, further experimental research will be conducted.

References

1) Beavers, G.S. and Joseph, D.D., Boundary conditions at a naturally permeable wall, *J. Fluid Mech.*, Vol. 30, pp. 197-207, 1967.
2) Wooding, R.A., Steady state free thermal convection of liquid in a saturated permeable medium, *J. Fluid Mech.*, Vol. 2, pp. 273-285, 1957.
3) Beckermann, C., Viskanta, R. and Ramadhyani, S., Natural convection in vertical enclosures containing simultaneously fluid and porous layer, *J. Fluid Mech.*, Vol. 186, pp. 257-284, 1988.
4) Hirsch, C., Numerical computation of internal and external flows, Vol. 2: Computational methods for inviscid and viscous flows, *J. Willey & Sons.*, 1990.
5) Welch, J.E., Harlow, F.H., Shannon J.P. and Daly B.J., The MAC method, A computing technique for solving viscous, incompressible, transient fluid-flow problems involving free surfaces, *Los Alamos Scientific Laboratory Report*, LA. 3425, 1966.
6) Rider, W.J. and Kothe, D.B., Reconstructing volume tracking, *J. Comput. Phys.*, Vol. 141, pp. 112-152, 1998.
7) Hirt, C.W. and Nichols, B.D., Volume of fluid (VOF) method for the dynamics of free boundaries, *J. Comput. Phys.*, Vol. 39, pp. 201-225, 1981
8) Hirt C.W. and Cook J.L., Calculating Three-Dimensional Flows around Structures and over Rough Terrain, J. *Comput. Phys.* Vol. 10, pp. 324-340, 1972.
9) Leonard B.P., A stable and accurate convective modeling procedure based on quadratic upstream interpolation, *Comp. Methods in Appl. Mech. Engrg.* 19(1), pp. 59-98, 1979.
10) Neuman S.P. and Witherspoon P.A., Analysis of nonsteady flow with a free surface using finite element method, *Water Resour. Res.*, Vol. 7, pp. 611-623, 1971.

(Received: April 15, 2005)